Analytical Model Validation of a Hybrid Precast Concrete Wall for Seismic Regions

B. J. Smith[1] and Y. C. Kurama[2]

[1]Department of Civil Engineering and Geological Sciences, University of Notre Dame, 156 Fitzpatrick Hall, Notre Dame, IN 46556; PH: (574) 631-5380; FAX: (574) 631-9236; email: bsmith24@nd.edu
[2]Department of Civil Engineering and Geological Sciences, University of Notre Dame, 156 Fitzpatrick Hall, Notre Dame, IN 46556; PH: (574) 631-5380; FAX: (574) 631-8377; email: ykurama@nd.edu

ABSTRACT

This paper presents an ongoing research project on the validation of "hybrid" precast concrete wall structures for use in seismic regions. Hybrid precast walls utilize a combination of mild (e.g., Grade 60) steel and high-strength unbonded post-tensioning (PT) steel for lateral resistance across horizontal joints. The mild steel reinforcement is designed to yield and provide energy dissipation. The unbonded PT steel provides self-centering capability to reduce the residual lateral displacements of the wall from a large earthquake. Both the PT steel and the mild steel contribute to the lateral strength, resulting in an efficient structure. The measured behavior of a 0.4-scale hybrid precast concrete wall test specimen is compared with an analytical model, focusing specifically on the applied lateral load and displacement, energy dissipation, behavior of the steel reinforcement, and behavior along the horizontal base-panel-to-foundation joint. The results from the analytical model were found to be consistent with the results from the testing of the wall.

INTRODUCTION AND BACKGROUND

As shown in Figure 1, the hybrid precast concrete wall system investigated in this research utilizes a combination of mild (e.g., Grade 60) steel and high-strength unbonded post-tensioning (PT) steel for lateral resistance across horizontal joints. The PT steel is provided by multi-strand tendons placed inside un-grouted ducts to prevent bond between the steel and concrete. Thus, the tendons are connected to the structure only at end anchorages. Under the application of lateral loads into the nonlinear range, the primary mode of displacement in these walls occurs through gap opening at the horizontal joint between the base panel and the foundation. Upon unloading, the PT steel provides a restoring force to close this gap, thus reducing the residual (i.e., permanent) lateral displacements of the wall after a large earthquake. The use of unbonded PT tendons delays the yielding of the strands and reduces the tensile stresses transferred to the concrete (i.e., reduced cracking) as the tendons elongate under lateral loading. The mild steel bars crossing the horizontal joint at the wall base are designed

to yield in tension and compression and provide energy dissipation through the gap opening/closing behavior. A pre-determined length of these bars is unbonded at the bottom of the base panel (by wrapping the bars) to prevent low-cycle fatigue fracture. Both the PT steel and mild steel contribute to the lateral strength of the wall, thus, resulting in an efficient structure.

Hybrid precast wall structures can offer high quality production, simpler construction, and excellent seismic characteristics. However, these walls are currently not allowed by ACI 318 (2008) unless their lateral performance is demonstrated through experimental evidence and analysis. To address this limitation, the primary objective of this ongoing research project at the University of Notre Dame is to experimentally and analytically validate hybrid wall structures for code approval according to the guidelines, prerequisites, and requirements in ACI ITG-5.1 (2007) and ACI 318. The specific project objectives are to develop: (1) a validated seismic design procedure for the hybrid precast wall system; (2) validated analytical models and design tools; and (3) practical guidelines and experimental evidence demonstrating the performance of these structures under lateral loading. In accordance with these objectives, the current paper compares the post-test analysis results with the measured behavior of a wall test specimen. The procedure that was used to design the specimen and the results from a pre-test analytical study can be found in Smith and Kurama (2009).

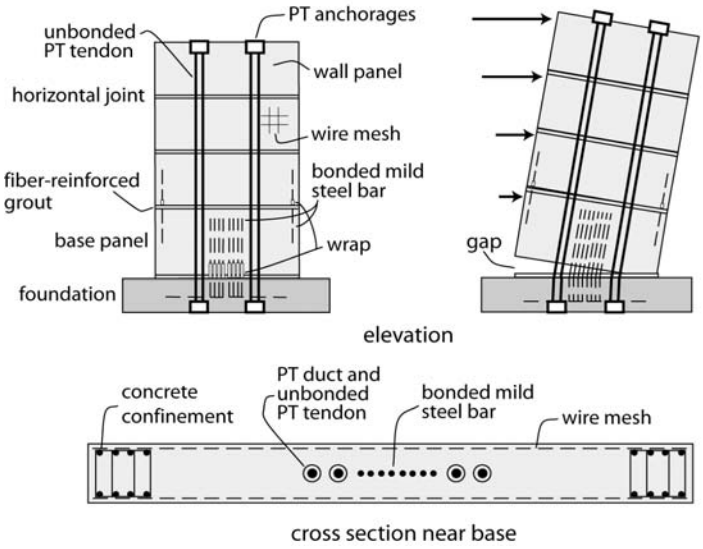

Figure 1. Elevation, Exaggerated Displaced Position, and Cross-Section of Hybrid Wall System

OVERVIEW OF VALIDATION AND TESTING REQUIREMENTS

The roadmap to the code validation of hybrid precast concrete walls is provided by ACI ITG-5.1, which lays out the minimum experimental evidence needed for the classification of these walls as "special" reinforced concrete (RC) shear walls based on ACI 318. Specific requirements are given with regards to the tested wall roof drift, Δ_w, measured wall lateral strength to the predicted strength ratio, PT strand stresses and strains, amount of energy dissipation, wall strength degradation, and shear slip along the horizontal joints, among other requirements. The design is conducted at two levels of wall drift as follows: (1) the design-level drift, Δ_{wd}, which is determined according to the requirements of ASCE 7 (2006); and (2) the validation-level drift, which is defined by ACI ITG-5.1 as:

$$\Delta_{wm} = 0.9\% \le 0.8\left(h_w / l_w\right) + 0.5 \le 3.0\% \quad (1)$$

where, h_w is the height to the top of the wall, and l_w is the length of the wall. The wall drift, Δ_w is defined as the lateral displacement at the top of the wall divided by the wall height. Prior to the validation testing, ACI ITG-5.1 requires that a pre-test design/analysis procedure for the specimen be established. A few key ACI ITG-5.1 requirements include: (1) the use of a minimum of two wall panels in the test structure (in order to model a representative panel-to-panel joint as well as the base-panel-to-foundation joint) unless the prototype structure uses a single panel for the full height of the wall; (2) a minimum specimen scale of one-third; (3) a minimum wall height-to-length aspect ratio of 0.5; and (4) the use of similar reinforcement details and representative building materials as in the full-scale prototype structure.

OVERVIEW OF TEST SET-UP, PROCEDURE, AND SPECIMEN

A photograph of the test specimen and a schematic of the test setup are shown in Figure 2. As described in Smith and Kurama (2009), the specimen was designed for a 4-story prototype parking garage with an approximate footprint of 42,000-sq-ft. The test was conducted at 0.4-scale, which satisfies the minimum scaling limit of ACI ITG-5.1. The lateral load was applied at the resultant location of the 1st mode inertial forces (12-ft from the wall base), resulting in a wall base moment to shear ratio of M_b/V_b=1.5l_w. An external downward axial load of about 73 kips was applied at the centerline of the wall at the top to simulate the gravity loads acting on the prototype structure. The test wall featured two panels: the base panel representing the 1st story and the upper panel representing the 2nd through 4th stories, thereby satisfying the ACI ITG-5.1 requirement for testing multi-panel walls. It was possible to model the upper story panels of the prototype wall as a single panel since the joints between these panels were designed not to have any significant gap opening.

For the subject test wall, the length, l_w, was 96-in, the height of the base panel, h_{pb}, was 57.5-in, and the wall panel thickness, t_w, was 6.25-in. The PT steel consisted of two tendons located 9-in north and south from the wall centerline. Each tendon included three 0.5-in diameter strands (design ultimate strength, f_{pu}=270-ksi) with an unbonded length from the top of the wall to the bottom of the foundation beam of about 18-ft. The average initial stress in the tendons, calculated from the measured strand forces prior to the application of the lateral load, was f_{pi}=0.55f_{pu}. The mild steel (i.e., energy dissipating steel) crossing the base joint consisted of four No. 6 bars (design yield strength, f_{sy}=65-ksi), with one pair of bars placed 6-in north and south from the wall centerline and the other pair 3-in north and south from the centerline. The energy dissipating bars were unbonded over a length of 10-in at the bottom of the base panel. Across the panel-to-panel joint, only two No. 6 bars were used, with one bar located at each end of the wall. This reinforcement was not designed to yield or dissipate energy, but to control any gap opening along the panel-to-panel joint. To prevent strain concentrations in the panel-to-panel joint reinforcement, a short 3-in length of the bars was unbonded at the bottom of the upper panel. The design unconfined concrete strength for the wall was 6.0-ksi and the design confined

concrete strength (within the toes of the base panel) was 9.1-ksi. However, the measured unconfined concrete strength for the base panel was only 4.8-ksi on the day that the wall was tested.

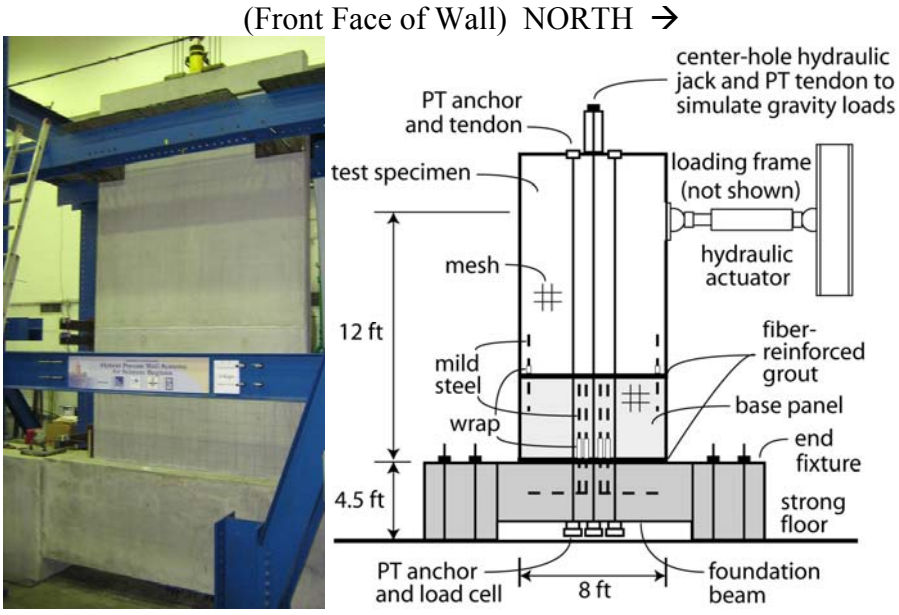

Figure 2. Test Set-Up: (a) Photograph; (b) Schematic Drawing

MEASURED BEHAVIOR OF SPECIMEN

Figure 3a shows the reversed-cyclic lateral displacement history that was used during the test, with three fully-repeated cycles at each displacement increment. The wall drift, Δ_w is defined as the relative lateral displacement of the wall between the lateral load location and the foundation divided by the height to the lateral load. The wall specimen was loaded in a slightly unsymmetrical manner due to the unexpected movement of the foundation during the test; however, all presented data in this paper have been corrected to isolate the wall response for this foundation movement. Figure 3b shows a photograph of the lower half of the wall during the third cycle at Δ_w=+1.90% (note the gap opening at the north end). The specimen sustained three cycles at a maximum positive drift (with the wall displaced southward) of Δ_w=+1.90% and a maximum negative drift of Δ_w=-1.55% prior to failure due to the crushing of the confined concrete at the toes. Figure 3c shows the south toe of the wall at the end of the test. It can be seen that the first confinement hoop was placed at a significant angle with the horizontal, resulting in a large region of unconfined concrete at the bottom of the base panel (at the east face of the panel, the first hoop was located 4.5-in from the bottom rather than the design location of 2-in). While not as extreme as the south toe, the hoop placement at the north toe was also misaligned. This misalignment of the confinement hoops, combined with the low unconfined concrete strength (4.8-ksi rather than the design strength of 6.0-ksi of the critical base panel), resulted in the failure of the wall at a lower drift level than expected.

Significant crushing of the wall concrete was not present until the final drift series of Δ_w=+1.90. The crushing of the confined concrete at the wall toes initiated at about Δ_w=+1.75%, after which the specimen started to undergo significant strength degradation. Additionally, while the design clear cover was 0.50-in for the welded wire fabric placed on each face of the wall panels, the actual clear cover was as little as 0.15-in near the south end of the base panel. As shown in Figure 3c, this resulted in the delamination of the wire fabric near the end of the test. Further discussion regarding the measured response of the specimen can be found in Smith and Kurama (2010).

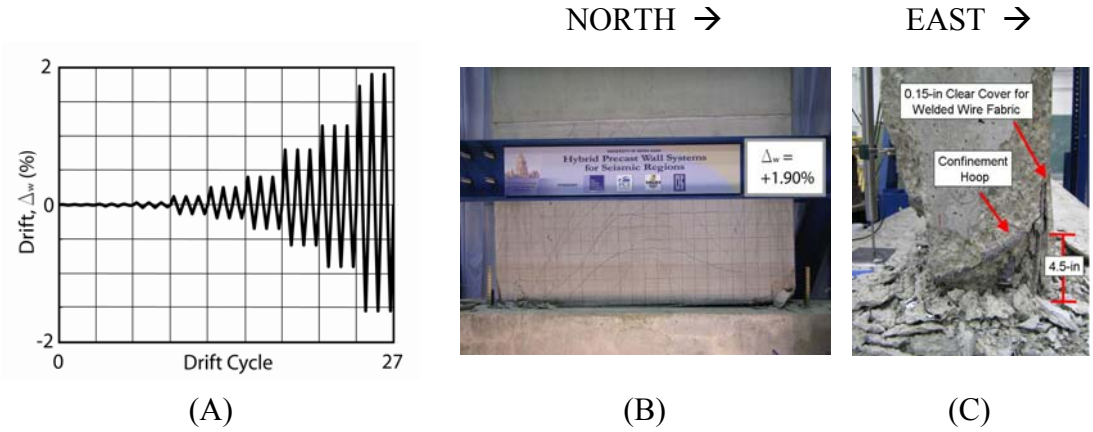

Figure 3. Wall Behavior: (a) Applied Displacement History; (b) Damage at Third Cycle of Δ_w=+1.90%; (c) South Toe of Wall after Completion of Test

POST-TEST VALIDATION OF ANALYTICAL MODEL

This section presents the post-test evaluation of an analytical model that was previously used in Smith and Kurama (2009) for the pre-test design validation of the test specimen. As described in Kurama (2002), the model uses the DRAIN-2DX Program (Prakash et al. 1993) as the analytical platform, with fiber beam-column elements to represent the precast concrete wall panels, and truss elements to represent the unbonded PT steel. Within the model structure, the unbonded portions of the mild steel reinforcement crossing the base-panel-to-foundation joint are placed outside of the concrete fiber cross-section to capture the uniform distribution of steel strains over the unbonded length. Gap opening at the wall base is modeled by assigning the tension strength of the concrete fibers at the bottom of the base panel to essentially zero. Note that different from the pre-test model in Smith and Kurama (2009), the analysis of the structure in this paper uses the actual, measured material and geometric properties of the wall. Slight modifications were made to the stiffness of the PT steel to account for the seating of

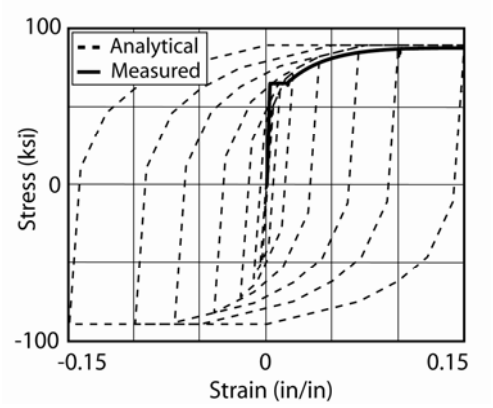

Figure 4. Mild Steel Model

the anchors and deformations of the foundation beam. Additionally, as shown in Figure 4, the cyclic stress versus strain behavior of the energy dissipating reinforcement was slightly modified from the measured monotonic behavior.

Lateral Load Versus Displacement Behavior. Figure 5 compares the experimental and analytical base shear force, V_b versus wall drift, Δ_w behaviors for the test specimen. As shown in Figure 5a, the maximum applied lateral load measured during the test was 120-kips, reached at Δ_w=+1.15%. The measured load at the design-level drift (Δ_{wd}=+0.40%) was 99-kips and at the failure-level drift (Δ_{wu}=+1.75%) was 114-kips. The failure-level drift was determined as the actual drift level reached when crushing of the confined concrete was first observed and, for the subsequent drift cycles, significant strength degradation occurred in the V_b-Δ_w behavior.

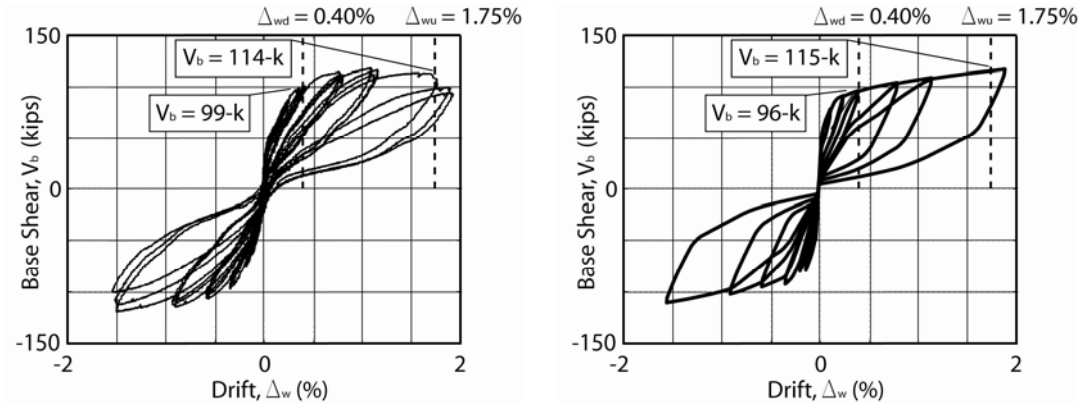

(A) (B)

Figure 5. V_b/Δ_w Behavior: (a) Measured; (b) Analytical

As shown in Figure 5b, the analytical model yields a similar load-displacement behavior with very comparable peak forces at both the early and late cycles. The estimated base shear is 96-kips at the design-level drift and 115-kips at the failure-level drift. The analytical model estimates slightly lower base shear forces than the measured forces during the earlier cycles. This may be explained by the fluctuating increases (between 2-kips and 8-kips) that occurred in the applied wall gravity load during these cycles. In the analytical model, the wall gravity load was held constant throughout the analysis, resulting in slightly lower base shear forces as compared with the test specimen. The fluctuations in the applied gravity load were prevented during the later cycles of the test. It can also be seen in Figure 5b that the analytical model is considerably stiffer than the measured behavior during the unloading of the wall. This occurred due to the discrepancies in the modeling of the Bauschinger effect during the unloading of the energy dissipating mild steel reinforcement at the wall base. It may be possible to improve the analytical estimations by using a better cyclic material model for the energy dissipating bars.

Energy Dissipation. As stated previously, the primary source of energy dissipation in the hybrid wall system develops through the reversed-cyclic yielding of the mild

steel reinforcement over the unbonded length of the bars as gap opening and closing occurs at the base-panel-to-foundation joint. To quantify the energy dissipation of the structure, ACI ITG-5.1 uses the energy dissipation ratio, β, which is defined as "the ratio of the measured energy dissipated by the test module during reversing cyclic displacements between given measured drift angles to the maximum theoretical energy that can be dissipated for the same drift angles." ACI ITG-5.1 requires that β be not less than 0.125 at the validation-level drift.

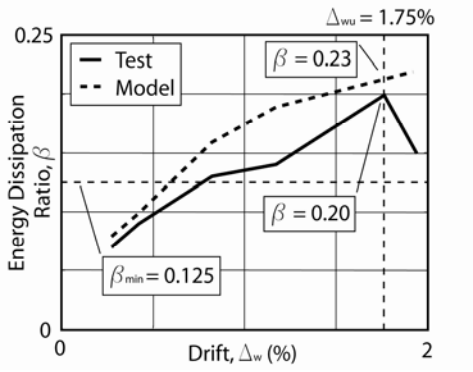

Figure 6. Energy Dissipation Ratio

The solid line in Figure 6 shows the measured energy dissipation ratio of the test structure plotted against the wall drift. The third cycle for each drift level was used to calculate the β ratios in this plot, except for the last series, where both the first and third cycles are shown. It can be seen that the specimen exceeded the minimum energy dissipation requirement at drift levels greater than Δ_w=+0.80% and achieved a maximum β ratio of 0.20 at Δ_{wu}=+1.75%. The strength degradation at the end of the test resulted in a reduction in β. The energy dissipation from the analytical model, shown by the dashed line in Figure 6, tends to overestimate the measured energy dissipation, especially during the intermediate drift levels. This is a consequence of the inadequacy of the model to accurately match the measured lateral stiffness of the wall during unloading.

Energy Dissipating Mild Steel Strains. Since the mild steel reinforcement crossing the base-panel-to-foundation joint serves as the main energy dissipater for the wall system, it is essential for these bars to yield before the design-level drift, but not fracture prior to the validation-level drift. Figure 7 shows the four mild steel bars at the bottom of the base panel prior to the placement of the concrete. The 10-in long plastic-wrapped unbonded length of the bars can be seen in the photograph, which was done to reduce the steel strains during the lateral displacements of the wall. Furthermore, the bars were located near the wall centerline to reduce the strains and, in turn, reduce the required unbonded length.

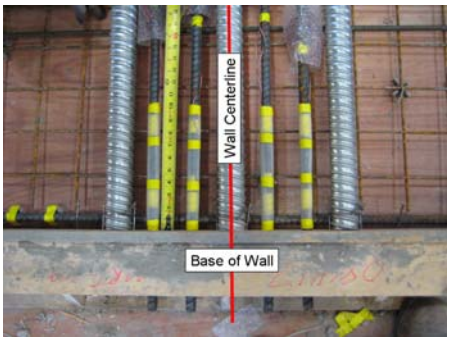

Figure 7. Placement and Unbonded Length of Mild Steel Bars Crossing Base Joint

Figure 8 compares the measured (using strain gauges placed within the unbonded length) and analytical strains of the middle two bars (referred to as the north intermediate and south intermediate bars) located +/-3-in from the wall centerline. As designed, the bars yielded (measured yield strain, ε_{sy}=0.00272-in/in)

relatively early in the test and prior to the design-level drift, Δ_{wd}=0.40%. The measured steel strains at Δ_{wd}=+0.40% were 0.006 and 0.012-in/in for the south and north intermediate bars, respectively, while the corresponding analytical strains were 0.012-in/in and 0.014-in/in. At the failure-level drift of Δ_{wu}=+1.75%, no strain measurements were possible due to gauge failure during the test. The analytical steel strains at Δ_{wu}=+1.75% were 0.048 and 0.057-in/in for the south and north intermediate bars, respectively. Variations in the measured and analytical strains may be related to the effective additional unbonded length that develops in the mild steel reinforcement under reversed-cyclic loading. In ACI ITG-5.2, it is assumed that this additional unbonded length is not present at the design-level drift but is present at the validation-level drift. For modeling purposes, the effective additional unbonded length was included throughout the analysis. As a result, the mild steel strains at the design-level drift may be slightly overestimated.

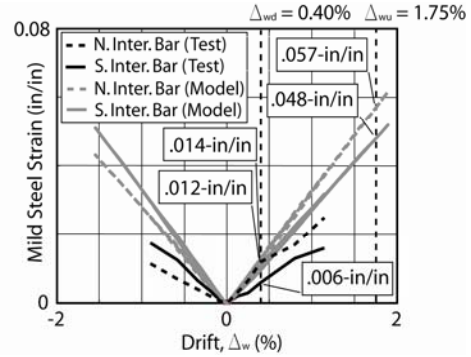

Figure 8. Measured and Analytical Strains in North and South Intermediate Mild Steel Bars

PT Steel Behavior. The PT steel provides the main restoring force for the wall, allowing the structure to return to its initial undisplaced position after being subjected to lateral loading. Figure 9a depicts this measured restoring force by plotting the

(A)

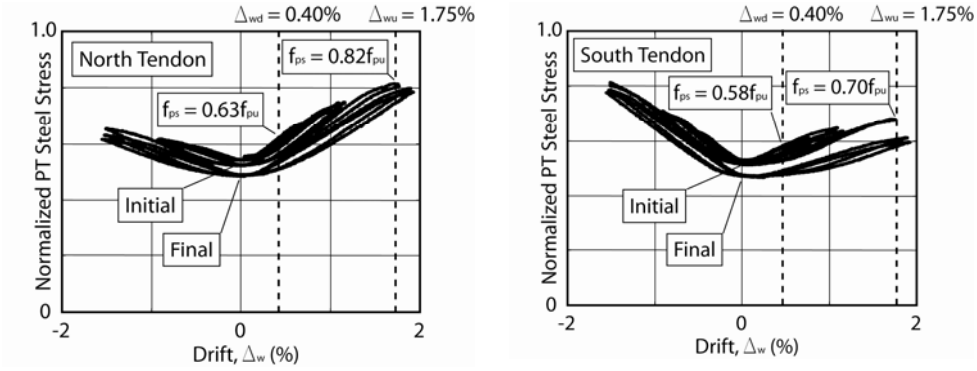

(B)

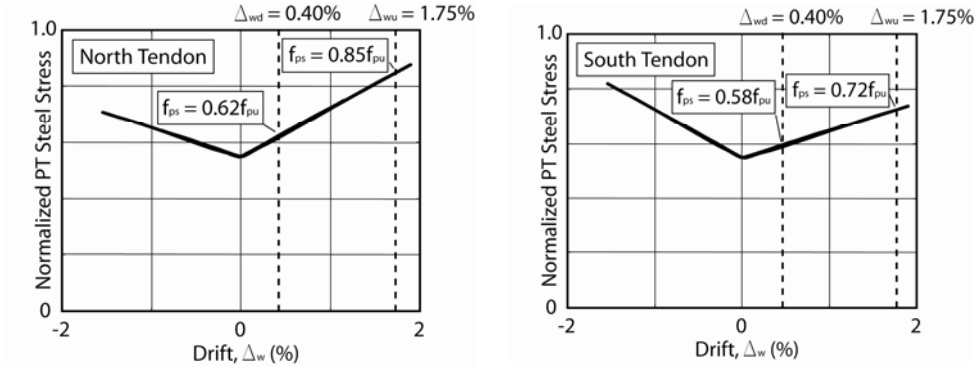

Figure 9. Average PT Steel Stresses: (a) Measured; (b) Analytical

normalized average stress in each of the north and south tendons (calculated as the sum of the measured strand forces divided by $A_p f_{pu}$, where A_p is the total area of the three 0.5-in diameter strands in each tendon and f_{pu}=270-ksi is the design strength of the strands). Consistent with the design expectations, the PT strands remained essentially linear-elastic throughout the test, which was made possible since the strands were unbonded over their entire length. Note that measured losses in the PT steel stresses can be seen during the second and third cycles to Δ_w=+1.90% in Figure 9a. These losses occurred due to the crushing of the concrete at the wall base (which resulted in a small amount of axial "shortening" of the wall), and not due to nonlinear straining of the strands.

From Figure 9a, the measured average stresses for the south and north tendons are 0.58 and 0.63f_{pu}, respectively, at the design-level drift, Δ_{wd}=+0.40%, and 0.70 and 0.82f_{pu}, respectively, at the failure-level drift, Δ_{wu}=+1.75%. Similar to the mild steel reinforcement, the differences in the north and south tendon stresses are due to the different elongations of the two tendons as the wall is displaced laterally. As shown in Figure 9b, the tendon stresses from the analytical model are very comparable to the measured data. The losses that occurred in the tendon stresses due to the crushing of the concrete at the wall base are not captured by the analytical model.

Gap Opening at Base-Panel-to-Foundation Joint. Consistent with the expected behavior of the wall, the structure opened a significant gap at the base-panel-to-foundation joint. The gap at the upper panel-to-panel joint was relatively small, with a maximum displacement of 0.06-in at the failure-level drift. Figure 10a shows the measured vertical size of the base gap at the extreme north and south toes of the wall. At the failure-level drift, Δ_{wu}=+1.75%, the north end gap opening was approximately 1.52-in. The analytical model results, shown in Figure 10b, compare well with the measured gap opening at both the design-level and failure-level drifts.

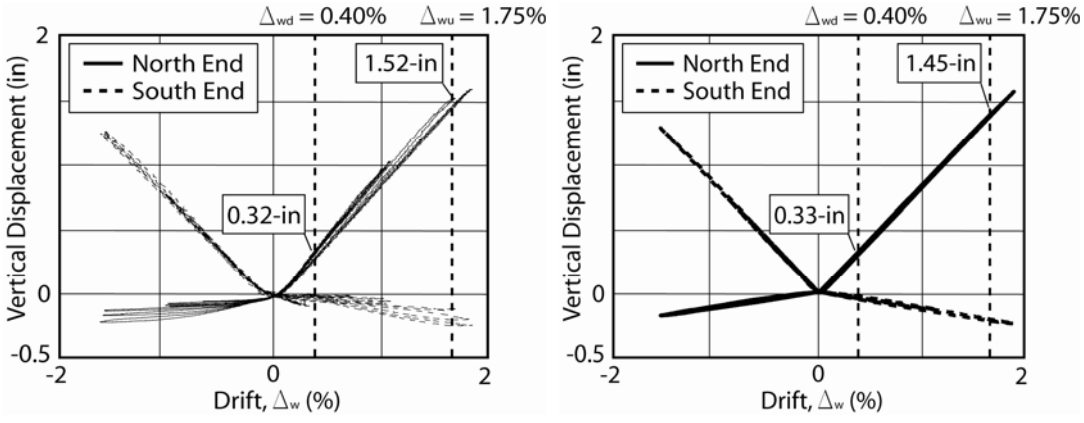

(A) (B)

Figure 10. Vertical Gap Opening Displacement at Wall Toes: (a) Measured; (b) Analytical

Vertical Displacement at Wall Top. The vertical displacement at the top of the wall is another measure that can be used to validate the analytical model. For this purpose,

the light solid line in Figure 11 shows the vertical displacement measured at the centerline of the wall at the location of the applied lateral load. The vertical displacement was about 0.08-in and 0.53-in at the design-level drift and failure-level drift, respectively. The results from the analytical model, shown with the dark dashed lines, compare well with the test results. The relatively small discrepancy between the measured and analytical displacements may be related to the discrepancies between the measured and analytical gap opening displacements at the base-panel-to-foundation and panel-to-panel joints. The axial shortening of the wall that occurred due to crushing of the concrete at the base is not captured by the analytical model.

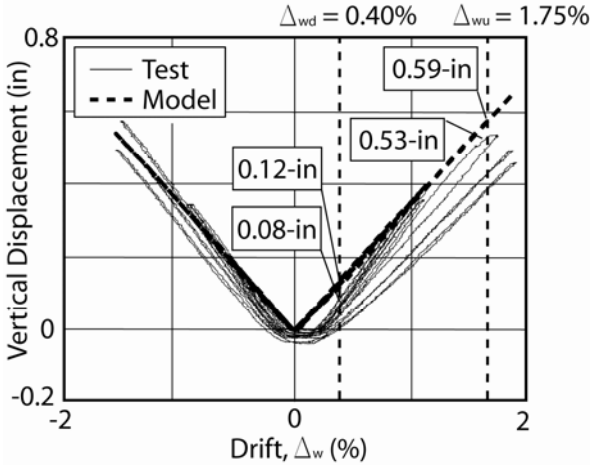

Figure 11. Vertical Displacements at Wall Top

SUMMARY AND CONCLUSION

This paper presents the results from an ongoing research project on the design, analysis, and behavior of hybrid precast concrete wall structures for seismic regions. The measured lateral performance of a 0.4-scale wall test specimen is compared with an analytical model that uses fiber elements. Overall, the wall system performed as designed; however, failure occurred prematurely due to lower than specified unconfined concrete strength and poor detailing/placement of the confinement hoops at the wall toes. The analytical model was able to replicate the overall load-displacement history and gap opening/closing behavior of the wall, as well as the behavior of the PT steel and mild steel reinforcement. The analytical lateral stiffness during the unloading of the wall was considerably stiffer than the measured stiffness, which resulted in the overestimation of the energy dissipated by the structure. It may be possible to improve the analytical estimations by using a better cyclic material model for the energy dissipating bars. The validation of the analytical model described in this paper allows the behavior of future test specimens to be predicted using similar modeling techniques.

ACKNOWLEDGMENTS

This research is funded by the Charles Pankow Foundation and the Precast/Prestressed Concrete Institute (PCI). Additional technical and financial support is provided by the High Concrete Group, LLC, the Consulting Engineers Group, Inc, and the University of Notre Dame. The authors would like to acknowledge the support of the PCI Research and Development Committee as well as the members of the Project Advisory Panel, who include Walt Korkosz (chair) of the

Consulting Engineers Group, Inc., Ken Baur of the High Concrete Group, LLC, Neil Hawkins of the University of Illinois at Urbana-Champaign, S.K. Ghosh of S.K. Ghosh Associates, Inc., and Dave Dieter of Mid-State Precast, LP. The authors would also like to thank Michael J. McGinnis from the University of Texas at Tyler for his assistance with data acquisition. Additional assistance and material donations have been provided by Julian Albrigo of ERICO International Corporation, Jenny Bass of Essve Tech Inc., Randy Ernest of Prestress Supply Inc., Eric Fries of Contractors Materials Company, Chris Lagaden of Ecco Manufacturing, Stan Landry of Enerpac Precision SURE-LOCK, Richard Lutz of Summit Engineered Products, Shane Whitacre of Dayton Superior Corporation, and Steve Yoshida of Sumiden Wire Products Corporation. Any opinions, findings, conclusions, and/or recommendations expressed in this paper are those of the authors and do not necessarily represent the views of the individuals or organizations acknowledged above.

REFERENCES

American Concrete Institute (ACI) Committee 318. (2008). *Building Code Requirements for Structural Concrete (ACI 318-08) and Commentary*, Farmington Hills, MI.

American Concrete Institute (ACI) Task Group 5. (2007). *ACI ITG-5.1: Acceptance Criteria for Special Unbonded Post-Tensioned Precast Structural Walls Based on Validation Testing and Commentary*, Farmington Hills, MI.

American Concrete Institute (ACI) Task Group 5. (2009). *ACI ITG-5.2: Requirements for Design of a Special Unbonded Post-Tensioned Precast Shear Wall Satisfying ACI ITG-5.1 and Commentary*, Farmington Hills, MI.

American Society of Civil Engineers (ASCE). (2006). *ASCE 7: Minimum Design Loads for Buildings and Other Structures*, Reston, VA.

Kurama, Y. (2002). "Hybrid Post-Tensioned Precast Concrete Walls for Use in Seismic Regions," *PCI Journal*, Vol. 47, Issue 5, pp.36-59.

Prakash, V., Powell, G. and Campbell, S. (1993). "DRAIN-2DX Base Program Description and User Guide; Version 1.10," *Report No. UCB/SEMM-93/17*, Department of Civil Engineering, University of California, Berkeley, CA.

Smith, B. and Kurama, Y. (2009). "Design of Hybrid Precast Concrete Walls for Seismic Regions." *ASCE 2009 Structures Congress*, Austin, TX.

Smith, B. and Kurama, Y. (2010). "Seismic Behavior of a Hybrid Precast Concrete Wall Specimen: Measured Response Versus Design Predictions." *9th U.S. National and 10th Canadian Conference on Earthquake Engineering*, Toronto, ON, Canada.